Preprints.org

Article

Not peer-reviewed version

Experimental Study of 3D Printing Cob-Based and Hemp-Based Material Mixtures for Home Building

Eden Binega *, Ali M. Memari , Girum Urgessa

Posted Date: 6 August 2026

doi: 10.20944/preprints202608.0409.v1

Keywords: sustainable and green infrastructure; 3D printing of houses; cob-material-based structures; hemp-material-based structures; automation in construction

Preprints.org is a free multidisciplinary platform providing preprint service that is dedicated to making early versions of research outputs permanently available and citable. Preprints posted at Preprints.org appear in Web of Science, Crossref, Google Scholar, Scilit, Europe PMC, OpenAlex.

Copyright: This open access article is published under a Creative Commons CC BY 4.0 license, which permit the free download, distribution, and reuse, provided that the author and preprint are cited in any reuse.

Preprints.org (www.preprints.org) | NOT PEER-REVIEWED | Posted: 6 August 2026 doi:10.20944/preprints202608.0409.v1

Disclaimer/Publisher's Note: The statements, opinions, and data contained in all publications are solely those of the individual author(s) and contributor(s) and not of MDPI and/or the editor(s). MDPI and/or the editor(s) disclaim responsibility for any injury to people or property resulting from any ideas, methods, instructions, or products referred to in the content.

Article

Experimental Study of 3D Printing Cob-Based and Hemp-Based Material Mixtures for Home Building

Eden Binega [1,*], Ali M. Memari [2] and Girum Urgessa [3]

[1] Department of Civil and Environmental Engineering and Department of Architecture, College of Engineering and Architecture, Howard University, Washington, DC 20059, USA
[2] Department of Architectural Engineering and Department of Civil and Environmental Engineering, The Pennsylvania State University, State College, PA 16802, USA
[3] Department of Civil and Environmental Engineering, College of Engineering and Architecture, Howard University, Washington, DC 20059, USA
* Correspondence: eden.yemesegen@howard.edu

Abstract

This paper presents an experimental study on extrudable cob-based and hemp-based materials, aiming to investigate their feasibility for 3D printing and their performance as sustainable construction materials. Cobcrete, a mixture of clay, sand, lime, straw, and water, and hempcrete, a composite material made from hemp hurd fiber and lime-based binders, have gained attention for their potential as a new construction material and possibly in 3D printing applications. The study focuses on assessing the workability, mechanical properties, and environmental sustainability aspects of these materials. A series of laboratory experiments are conducted to evaluate the printability, compressive strength, flexural strength, and water absorption characteristics of the extruded cobcrete and hempcrete specimens. Additionally, the impact of different mix ratios and curing conditions on the material performance is examined. The findings reveal that both cobcrete and hempcrete exhibit favorable printability potential and demonstrate promising mechanical properties suitable for construction applications. Moreover, these materials showcase sustainability advantages, including low embodied energy and potential carbon sequestration for hempcrete. The study contributes to the understanding of the feasibility and performance of 3D printable cobcrete and hempcrete, providing insights into their potential as eco-friendly alternatives in the construction industry. The results underscore the need for further research and development to optimize these materials for broader adoption and to address challenges such as standardization, regulatory compliance, and market acceptance. Ultimately, this study paves the way for utilizing 3D printable cobcrete and hempcrete in sustainable construction practices, contributing to the development of greener and more environmentally conscious building technologies.

Keywords: sustainable and green infrastructure; 3D printing of houses; cob-material-based structures; hemp-material-based structures; automation in construction

1. Introduction

1.1. Background on 3D Printable Cobcrete and Hempcrete Materials

3D printable cobcrete and hempcrete materials are innovative approaches in the field of sustainable construction. These materials combine traditional building techniques with modern 3D printing technology to create environmentally friendly alternatives for construction applications [1]. Cobcrete is a blend of cob, a mixture of clay, sand, straw, and concrete additives. Cob has been used as a building material for centuries due to its availability and ease of construction. By incorporating concrete additives, such as binders or admixtures, cobcrete gains enhanced strength, durability, and workability, making it suitable for 3D printing processes [2,41]. Hempcrete, on the other hand, is a

© 2026 by the author(s). Distributed under a Creative Commons CC BY license.

Preprints.org (www.preprints.org) | NOT PEER-REVIEWED | Posted: 6 August 2026 doi:10.20944/preprints202608.0409.v1

composite material made from hemp fibers and lime-based binders. Hemp fibers are derived from the stalks of industrial hemp plants, which are known for their rapid growth and sustainability. Lime-based binders, such as lime and/or hydraulic lime, are combined with the hemp fibers to create a lightweight and insulating material.

Both 3D printable cobcrete and hempcrete offer several benefits in terms of sustainability and eco-friendliness. Firstly, these materials have a low carbon footprint due to the use of natural and renewable resources [3]. As a crop, hemp absorbs significant amounts of carbon dioxide during its growth, making hempcrete a carbon-negative material [20]. Additionally, cobcrete and hempcrete reduce the need for energy-intensive manufacturing processes associated with conventional construction materials such as masonry, concrete, or steel. Moreover, these materials exhibit good thermal insulation properties, promoting energy efficiency and reducing the need for heating and cooling systems in buildings [21]. They also provide good breathability, allowing for the regulation of moisture and improving indoor air quality.

The integration of 3D printing technology with cobcrete and hempcrete opens up possibilities for complex and customizable designs, rapid construction, and reduced material waste. These materials can be extruded through a 3D printer nozzle, layer by layer, to create structures with intricate geometries and precise dimensions [4,5].

While 3D printable cobcrete and hempcrete materials show promise, further research and development are still needed to optimize their properties, address challenges related to their structural strength and durability, and establish standards and regulations for their use in construction projects. Nonetheless, their potential to contribute to sustainable and environmentally conscious building practices makes them an exciting area of exploration in the field of construction materials.

1.2. Significance of the Study

The significance of the study presented here lies in its exploration and evaluation of the feasibility and performance of cobcrete and hempcrete as sustainable construction materials for 3D printing applications. The study addresses several important aspects:

1. **Feasibility and Performance:** The study investigates the workability and mechanical properties of cobcrete and hempcrete. It assesses their printability, compressive strength, flexural strength, and tensile strength through laboratory experiments. By doing so, the study provides evidence of the materials' performance and their suitability for construction applications.
2. **Sustainable Construction Materials:** Cobcrete and hempcrete are eco-friendly alternatives to traditional construction materials [22]. Cobcrete utilizes clay, sand, straw, and concrete additives, while hempcrete is a composite material made from hemp fibers and lime-based binders [24]. Both materials exhibit promising sustainability advantages, such as low embodied energy and potential carbon sequestration for hempcrete [23]. By highlighting these benefits, the study contributes to the development of greener and more environmentally conscious building technologies.
3. **Potential for 3D Printing:** The study specifically focuses on the potential of cobcrete and hempcrete for 3D printing applications. 3D printing offers advantages in terms of efficiency, customization, and reduced waste in construction [25]. By evaluating the printability of these materials and their mechanical properties, the study explores their viability for 3D printing processes.
4. **Further Research and Development:** The study acknowledges that while cobcrete and hempcrete show promise, further research and development are necessary to optimize these materials for broader adoption. The study identifies challenges such as standardization, regulatory compliance, and market acceptance that need to be addressed. This recognition underscores the need for continued efforts to refine these materials and enhance their practical implementation in the construction industry.

© 2026 by the author(s). Distributed under a Creative Commons CC BY license.

Preprints.org (www.preprints.org) | NOT PEER-REVIEWED | Posted: 6 August 2026 doi:10.20944/preprints202608.0409.v1

In summary, this study contributes to the understanding of the feasibility, performance, and sustainability aspects of 3D printable cobcrete and hempcrete materials. Its findings provide valuable insights into the potential of these materials as eco-friendly alternatives in construction, paving the way for the development of greener and more sustainable building technologies.

1.3. Objectives of the Study

The first objective of the study is to determine the appropriate amount of ingredients required for cobcrete and hempcrete materials. This involves carefully selecting and preparing the necessary components, including clay, sand, straw, concrete additives, hemp fibers, and lime-based binders. By achieving the optimal mix ratios, the study aims to ensure the desired material composition for subsequent testing and analysis.

The second objective is to establish the fundamental printing parameters and settings that align with the unique material properties of cobcrete and hempcrete. This step is crucial to ensure compatibility between the printing process and the characteristics of the materials being used. Parameters such as nozzle size, temperature, and layer height will be determined to facilitate successful 3D printing of cobcrete and hempcrete structures.

The third objective revolves around analyzing the mechanical properties of cobcrete and hempcrete. Specifically, the study aims to evaluate the mechanical characteristics of novel mix ratios developed for these materials. Compressive strength, flexural strength, and water absorption characteristics will be assessed to determine the performance and durability of the materials in construction applications.

The final objective of the study is to evaluate the overall performance and feasibility of 3D printed cobcrete and hempcrete. This evaluation encompasses multiple aspects, including printability, structural integrity, and suitability for construction. By conducting rigorous laboratory experiments, the study aims to provide empirical evidence of the materials' capabilities and identify potential areas for improvement.

The objectives of the study involve ingredient selection and preparation, establishment of printing parameters, analysis of mechanical properties, and evaluation of the performance and feasibility of 3D printed cobcrete and hempcrete materials. These objectives pave the way for a comprehensive understanding of the potential applications and advantages of these sustainable construction materials in the context of 3D printing technology.

1.4. Chapter Organization

The remainder of the paper is organized as follows. Section 2.1 explains the methodology of preparing the mix ratio of cobcrete and hempcrete materials. Sections 2.2 and 2.3 discuss the experimental setup and printing parameters for the 3D printing process. Testing procedures for physical and mechanical properties of the materials are elaborated in Section 2.4, which covers specific gravity, compressive strength, splitting tensile strength, and three-point bending flexure tests. Section 2.5 presents the procedure for preparation of manual 3D printing. Section 3 presents the results and discussion of the experimental outcomes. Moreover, Section 3 discusses improved mixture designs to achieve a printable and buildable structure. Finally, Section 4 concludes the paper by presenting a summary, limitations, and future work.

2. Methodology

2.1. Selection and Preparation of Cobcrete and Hempcrete Materials

In this research, cobcrete and hempcrete are introduced as sustainable building materials that are selected to be modernized and perhaps adapted for 3D printing of houses. These materials are cost-effective, naturally insulated, and environmentally friendly. Even though the existing 3D

© 2026 by the author(s). Distributed under a Creative Commons CC BY license.

Preprints.org (www.preprints.org) | NOT PEER-REVIEWED | Posted: 6 August 2026 doi:10.20944/preprints202608.0409.v1

printing technology challenges of buildability, printability, and skilled worker needs are still going to continue to be encountered, 3D printing of cob- and hemp-based structures is possible [11,26].

Cob- and hemp-based construction are favorable under compressive load or stress resistance mechanisms [11]. In spite of the tensile load or stress resistance coming from the straw in cob-based material and the hemp fiber and hurd in hemp-based material, it is still crucial to consider using other tensile load or stress resisting materials in building the whole 3D printed house. Bamboo is selected as the typical sustainable material that can contribute to resisting tensile load or stress in this study of 3D printed house construction [42,43].

2.1.1. Mixture Design of Cobcrete

The greatest challenge of building with cob is that modern building techniques rely heavily on touch and feel, instead of quantifiable measurements. In the field, sand and clay are mixed together with various ratios and then water is added until the material "feels right." The procedure used for mixing, molding, and curing is as follows.

1. The initial mixture of soil, sand, and water was done in a concrete mixer to increase efficiency. Alternatively, dry mix first, and then add water. N.B.: To determine if the mix was at the appropriate moisture level, a handful of the mix was taken out of the concrete mixer and compacted into a handful-sized ball. The ball was then thrown up two to three feet in the air four times [18].
2. If the ball was able to hold together when caught, the mix was ready to have straw added. The mixture of soil, sand, and water was then placed onto a tarp. The straw was manually integrated by coating the sand and soil with straw and then stomping the straw into the mix [27]. From there the mix was rolled and folded. More straw was used to coat the batch, and this process was repeated until the entirety of the straw was integrated evenly throughout the batch.
3. Once the mixture was complete, the cob was then manually formed into molds of the specimens into cubes, cylinders, and beams.
4. After molding into cube, cylinder, and beam shapes, the specimens were put on a vibrating table to help settle the mixture well in the mold.
5. After 24 h of keeping the specimen at room temperature, the cube molds were removed. However, for the rectangular beams and the cylinders, the molds were removed, respectively, after 6 days and 14 days of keeping in room temperature, as they were too wet to be removed earlier.
6. The specimens were kept at room temperature until the day of testing.

The cast samples included nine cubes, three cylinders, and three rectangular beams prepared, respectively, to test for compressive, tensile, and flexural strength. In general, whenever testing for specimen strength, it is always advised to make and test three specimens from the same mix. This is done to reduce or average out the error due to manually introduced differences among the three specimens. The compressive strength tests of 7-day-old specimens are known to result in 65% (or 70%) of the strength of the 28-day-old specimens (99% of the strength) [19,28].

Different mix ratios of cobcrete were designed by varying the amount of clay, sand, lime, water, superplasticizer, and straw content in the mixture in order to understand the workability and strength of the mixture for 3D printing. The first trial started with 23% clay, 55% sand, 3% lime, 17% water, 1% straw, and 1% superplasticizer [29]. Increasing the amount of clay content decreases the workability of the mixture, requiring more water content. Figure 1 shows various mixture designs of cobcrete.

© 2026 by the author(s). Distributed under a Creative Commons CC BY license.

Preprints.org (www.preprints.org) | NOT PEER-REVIEWED | Posted: 6 August 2026 doi:10.20944/preprints202608.0409.v1

Specimens with Clay and Sand Amount Variation

Increased to 6.974 kg due to less workability

Specimens	CS-1 (%)	kg
Clay (%)	23	5.750
Sand (%)	55	13.750
Lime (%)	3	0.750
Water (%)	17	4.250
Straw (%)	1	0.250
Superplasticizer (%)	1	0.250
Cement (%)		
Total	100	25.000
	Total	**25**

Specimens	CS-2 (%)	kg
Clay (%)	43	10.750
Sand (%)	35	8.750
Lime (%)	3	0.750
Water (%)	17	4.250
Straw (%)	1	0.250
Superplasticizer (%)	1	0.250
Cement (%)		
Total	100	25.000
	Total	**25**

Specimens	CS-3 (%)	kg
Clay (%)	63	15.750
Sand (%)	15	3.750
Lime (%)	3	0.750
Water (%)	17	4.250
Straw (%)	1	0.250
Superplasticizer (%)	1	0.250
Cement (%)		
Total	100	25.000
	Total	**25**

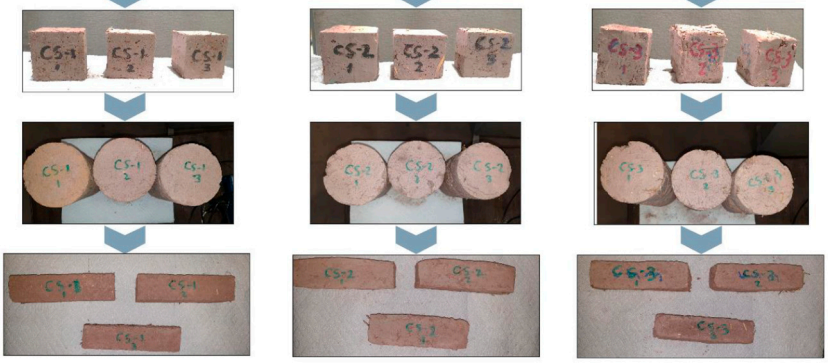

(a)

Specimens with Water Amount Variation

Specimens	W-1	kg
Clay (%)	24	6
Sand (%)	56	14
Lime (%)	3	0.75
Water (%)	15	3.75
Straw (%)	1	0.25
Superplasticizer (%)	1	0.25
Cement (%)		0
Total	100	25
	Total	**25**

Specimens	W-2	kg
Clay (%)	22	5.5
Sand (%)	54	13.5
Lime (%)	3	0.75
Water (%)	19	4.75
Straw (%)	1	0.25
Superplasticizer (%)	1	0.25
Cement (%)		0
Total	100	25
	Total	**25**

(b)

© 2026 by the author(s). Distributed under a Creative Commons CC BY license.

Preprints.org (www.preprints.org) | NOT PEER-REVIEWED | Posted: 6 August 2026 doi:10.20944/preprints202608.0409.v1

Specimens with Superplasticizer Amount Variation

Specimens	SP-1	kg
Clay (%)	23	5.75
Sand (%)	54.5	13.625
Lime (%)	3	0.75
Water (%)	17	4.25
Straw (%)	1	0.25
Superplasticizer (%)	1.5	0.375
Cement (%)		0
Total	100	25
	Total	**25**

Specimens	SP-2	kg
Clay (%)	23.5	5.875
Sand (%)	55	13.75
Lime (%)	3	0.75
Water (%)	17	4.25
Straw (%)	1	0.25
Superplasticizer (%)	0.5	0.125
Cement (%)		0
Total	100	25
	Total	**25**

(c)

Specimens with 3 % Cement Addition

Specimens	C-1	kg
Clay (%)	22	5.5
Sand (%)	53	13.25
Lime (%)	3	0.75
Water (%)	17	4.25
Straw (%)	1	0.25
Superplasticizer (%)	1	0.25
Cement (%)	3	0.75
Total	100	25
	Total	**25**

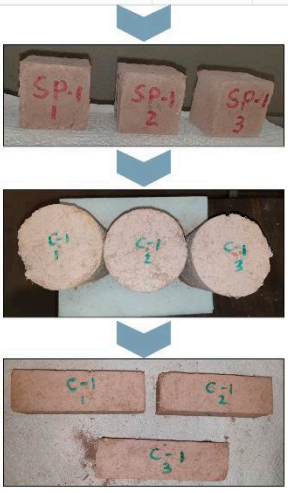

(d)

Figure 1. Cobcrete specimens with (**a**) sand amount variation, (**b**) water amount variation, (**c**) superplasticizer amount variation, and (**d**) 3% cement addition.

© 2026 by the author(s). Distributed under a Creative Commons CC BY license.

Preprints.org (www.preprints.org) | NOT PEER-REVIEWED | Posted: 6 August 2026 doi:10.20944/preprints202608.0409.v1

2.1.2. Mixture Design of Hempcrete

As shown in Figure 2, three different hempcrete mixture designs were tested for mechanical strength and printability. All the ingredients in the mix ratio design, including lime, water, and hemp, were varied as shown in the figure. Mixing, casting, and curing of the hempcrete mixture follows the procedure outlined below [6,30].

1. Hemp was added to the mixing vessel.
2. Lime binder was added slowly, folding and dry mixing it into the hemp by hand. It took 1–2 min.
3. Once mixed uniformly, 75–80% of the water volume was added slowly [32]. It was then mixed for about 4 min.
4. The remaining water was added slowly and deliberately. It was then mixed for 1 min. The mix should be consistent and feel like damp wood chips flowing freely.
5. Finally, the mix was cast in cube, cylinder, and beam molds. N.B.: Compaction is key when casting hempcrete [31].
6. The molds were removed after 24 h for the cubes and beams, whereas for the cylinders they were removed after 3 days.
7. After the specimens were demolded, they were kept at room temperature until the day of testing.

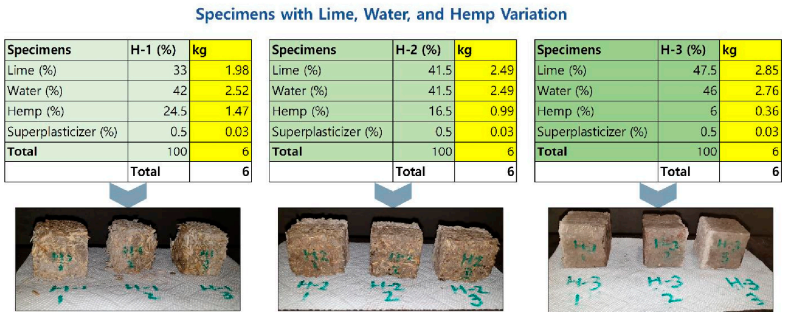

Figure 2. Hempcrete specimens with lime, water, and hemp variations.

2.2. Experimental Setup for 3D Printing

In order to test the mechanical strength of cobcrete and hempcrete, a printing robotic arm, raw material mixer, and pump and its controller were used, as shown in Figure 3. For both cobcrete and hempcrete, the general procedure for testing the material mechanical strength and printability is similar. The initial step is to mix the raw material in a mixer. Then the consistency of the mix is checked before casting the cube, cylinder, and rectangular beam specimens. To check the printability, a manual printing pump was used. The void and crack initiation of the mix were checked through a thermal image. Figures 4 and 5 show the general procedure of cobcrete and hempcrete testing, respectively.

Figure 3. 3D printing experimental setup.

© 2026 by the author(s). Distributed under a Creative Commons CC BY license.

Preprints.org (www.preprints.org) | NOT PEER-REVIEWED | Posted: 6 August 2026 doi:10.20944/preprints202608.0409.v1

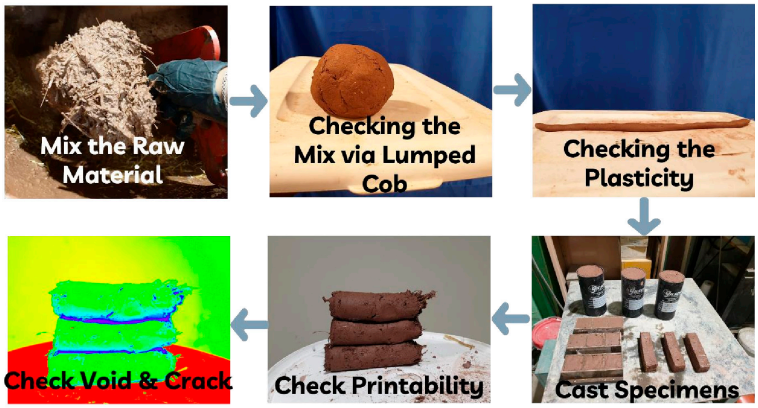

Figure 4. Procedure for "cobcrete" testing.

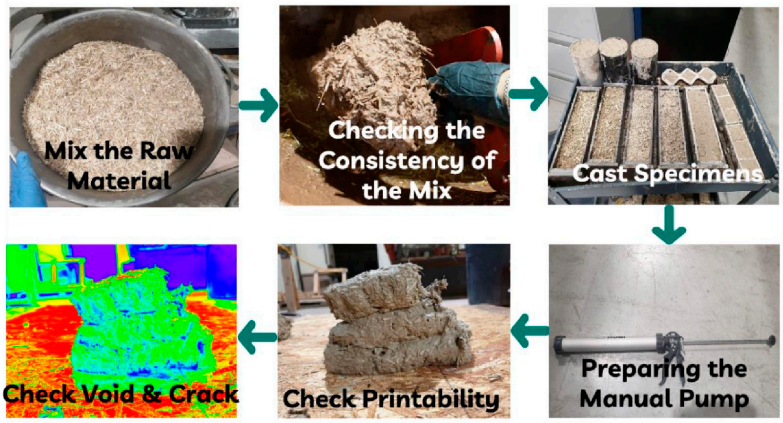

Figure 5. Procedure for hempcrete testing.

2.3. Printing Parameters and Settings

The printing parameters exhibit strong reliance on both the robotic nozzle and pump components [7]. Within the robotic nozzle, these parameters encompass the nozzle speed and diameter. Meanwhile, the pump component is characterized by the extrusion rate parameter. The meticulous specifications for the bead width and layer height in the 3D printed structure hold paramount significance. These pivotal parameters find their genesis in the original G-code file of the 3D model, allowing for their initial control. The term "bead width" denotes the dimension of the 3D printed structure as observed from a top-down or horizontal perspective [33]. On the other hand, "layer height" pertains to the vertical thickness of the 3D printed structure when viewed from a lateral or vertical standpoint [34]. Table 1 details the specific 3D printing parameters employed during the printing process, encompassing robotic nozzle speed, pump extrusion rate, nozzle diameter, bead width, and layer height. For enhanced clarity, the precise definitions of bead width and layer height are visually depicted in Figure 6.

Table 1. 3D printing parameters.

3D Printing Parameter	Value
Robotic nozzle speed	50–65% of 150 mm/s
Pump extrusion rate	7.8 L/min
Nozzle diameter	38 mm
Bead width	40–42 mm
Layer height	20–21 mm

© 2026 by the author(s). Distributed under a Creative Commons CC BY license.

Preprints.org (www.preprints.org) | NOT PEER-REVIEWED | Posted: 6 August 2026 doi:10.20944/preprints202608.0409.v1

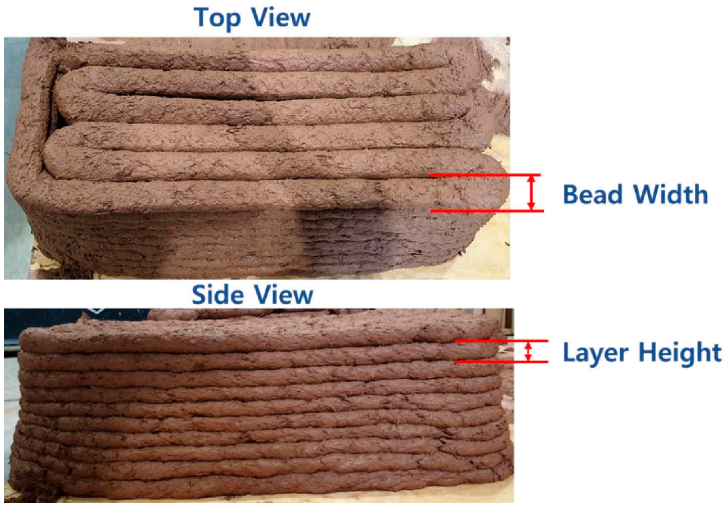

Figure 6. Bead width and layer height of 3D printed sample.

2.4. Testing Procedures for Physical and Mechanical Properties

The first physical properties checked in this study included the specific gravity or density of each ingredient used in cobcrete and hempcrete. The density of these materials affects the weight and structural properties. Cob- and hemp-based construction are favorable under compressive load or stress resistance mechanisms [11]. In spite of the tensile load or stress resistance coming from the straw in cobcrete and the hemp hurd/fiber in hempcrete, it is still crucial to consider using other tensile load or stress resisting materials in the components made up of these materials in the construction of buildings (houses) using 3D printing [15–17]. Bamboo is selected as the typical sustainable material that can contribute to resisting tensile load or stress in this study of 3D printed house construction [42].

2.4.1. Specific Gravity Test of Cobcrete and Hempcrete

The density of cobcrete can vary widely based on the proportions of clay, sand, straw, and concrete used in the mixture. The typical density range is approximately 1600 kg/m^3 to 2000 kg/m^3 [8,9]. Hempcrete is known for being relatively lightweight compared to cobcrete due to the low density of hemp fibers and the porous nature of the mixture [35]. The typical density range is approximately 200 kg/m^3 to 600 kg/m^3. These density ranges can vary depending on factors such as the exact mixture ratios, compaction methods, curing conditions, and the specific types of materials used. In order to get an accurate value of the specific gravity of the materials used during the experiment conducted at Penn State, the weight of each material was measured, as presented in Figure 7, initially with a consistent measuring jar of 14 oz and cylinder of 400 mL, as shown in Table 2.

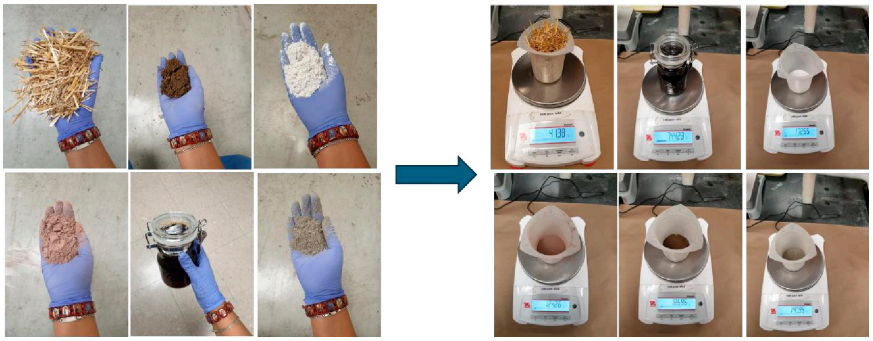

Figure 7. Measuring process of specific gravity.

© 2026 by the author(s). Distributed under a Creative Commons CC BY license.

Preprints.org (www.preprints.org) | NOT PEER-REVIEWED | Posted: 6 August 2026 doi:10.20944/preprints202608.0409.v1

Table 2. Specific gravity of each ingredient.

Density Calculation	Mass (g)	Mass (g)	Density (g/L)
Measuring Cylinder (400 mL)	26.62		
Measuring Jar (14 oz)	332.73		
Lime + Cylinder (/100 mL)	172.55	Lime (/100 mL): 145.93	1459.3
Straw + Cylinder (/400 mL)	41.38	Straw (/400 mL): 14.76	36.9
Sand + Cylinder (/100 mL)	186.96	Sand (/100 mL): 160.34	1603.4
Cement + Cylinder (/100 mL)	140.96	Cement (/100 mL): 114.34	1143.4
Clay + Cylinder (/100 mL)	124.27	Clay (/100 mL): 97.65	976.5
Superplasticizer + Jar (/14 oz)	744.23	Superplasticizer (/14 oz): 411.5	993.9
Water	—	Water	1000

2.4.2. Compressive Strength Test of Cobcrete

Three "cobcrete" cube samples were tested after the 7th day, 14th day, and 28th day, which required having a total of nine different cast pieces. The compressive strength was tested according to ASTM-C109/C109M [10,11].

The loading rate used in the testing machine was 150 lbF/min. From the testing machine, three basic raw data points were collected, including displacement, force, and time. Using the displacement and load data points, a Load-Displacement scattered graph is plotted for three different cubes for each specimen, as shown in Figure 10. The three graphs are then plotted together to find the average result, as shown in Figure 11. Finally, by dividing the force by the cross-sectional area of the specimens, the Compressive Strength-Displacement graph is plotted, as shown in Figures 12–14 for the 7th, 14th, and 28th days of testing. In addition, Figures 8 and 9 show the test setup and the fractured "cobcrete" specimen, respectively.

Figure 8. "Cobcrete" compression test setup.

© 2026 by the author(s). Distributed under a Creative Commons CC BY license.

Preprints.org (www.preprints.org) | NOT PEER-REVIEWED | Posted: 6 August 2026 doi:10.20944/preprints202608.0409.v1

Figure 9. Fractured "cobcrete" specimen.

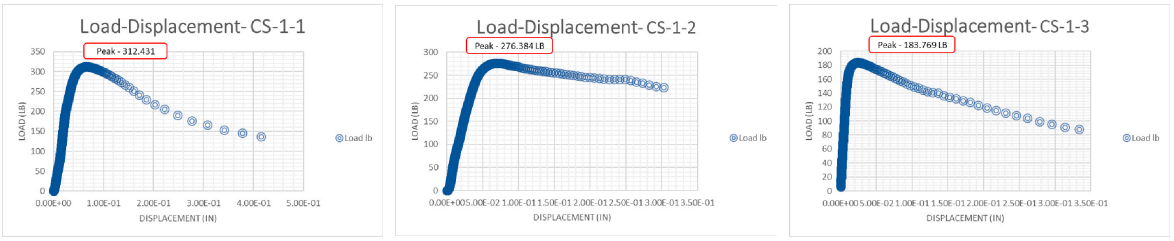

(1) **(2)** **(3)**

Figure 10. "Cobcrete" Load-Displacement graph (CS-1 specimens 1–3).

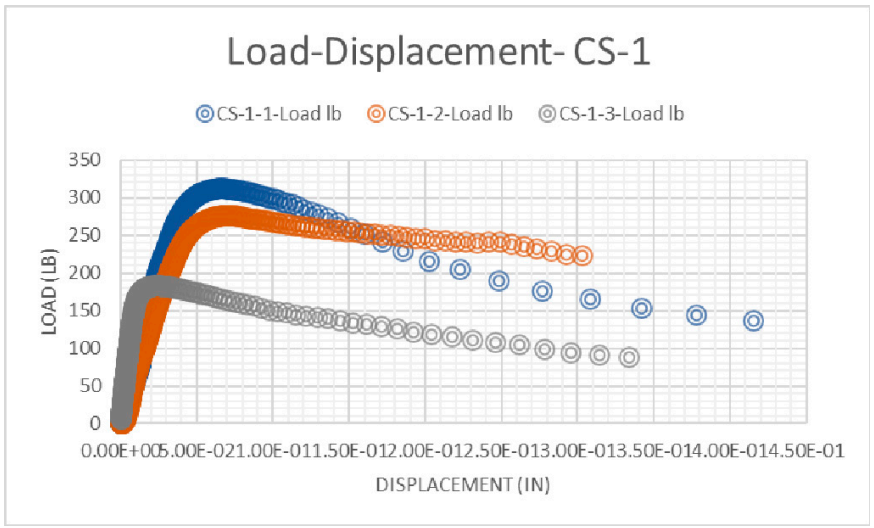

Figure 11. "Cobcrete" combined Load-Displacement graph.

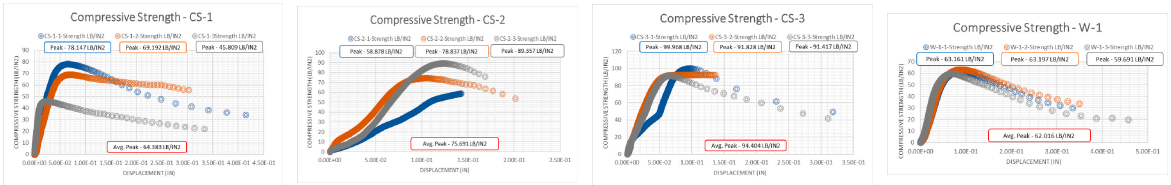

(CS-1) **(CS-2)** **(CS-3)** **(W-1)**

© 2026 by the author(s). Distributed under a Creative Commons CC BY license.

Preprints.org (www.preprints.org) | NOT PEER-REVIEWED | Posted: 6 August 2026 doi:10.20944/preprints202608.0409.v1

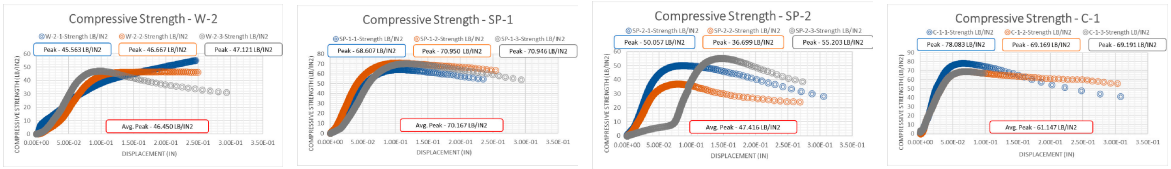

(W-2) (SP-1) (SP-2) (C-1)

Figure 12. "Cobcrete" 7th day compressive strength graph of various mixes.

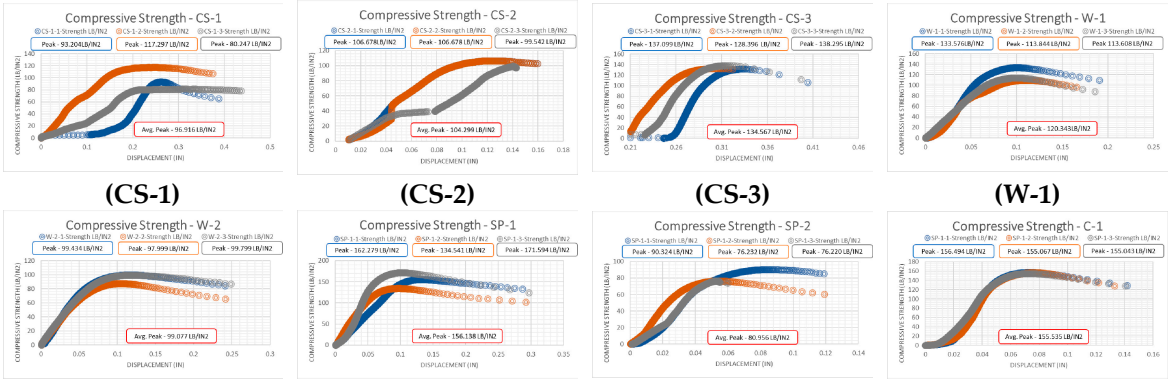

(CS-1) (CS-2) (CS-3) (W-1)

(W-2) (SP-1) (SP-2) (C-1)

Figure 13. "Cobcrete" 14th day compressive strength graph of various mixes.

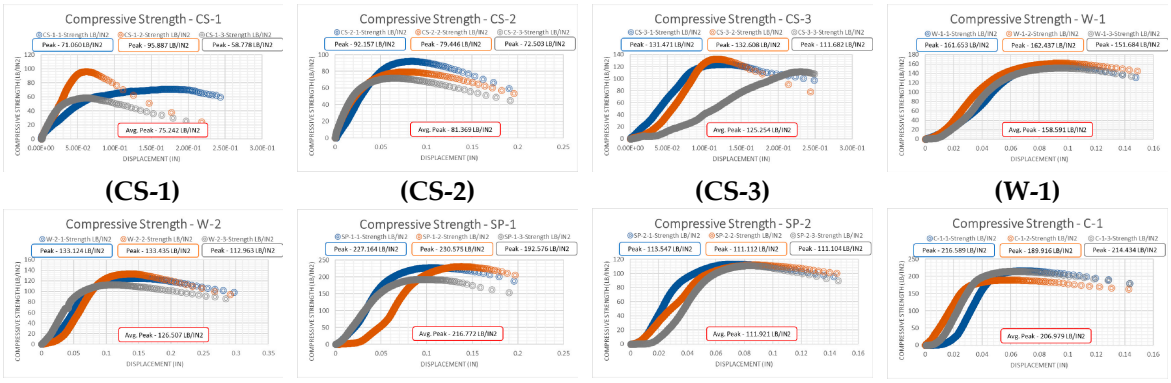

(CS-1) (CS-2) (CS-3) (W-1)

(W-2) (SP-1) (SP-2) (C-1)

Figure 14. "Cobcrete" 28th day compressive strength graph of various mixes.

2.4.3. Splitting Tensile Test of Cobcrete

The cobcrete cylinders were tested for tensile strength on the 28th day. For each specimen type, three samples were cast. The cylinders' tensile strength was tested according to ASTM-C496/C496M [10,11].

The loading rate used in the testing machine was 150 lbf/min [38]. From the testing machine, three types of basic raw data were collected, namely, displacement, force, and time. Using the displacement and load data points, a Load-Displacement scattered graph is plotted for three different specimen cylinders, as shown in Figure 17. Finally, by using Equation (1), the Tensile Strength-Displacement graph is plotted, as shown in Figure 18, by combining the three graphs of the three different samples of a specimen. Figures 15 and 16 show the test setup and the fractured "cobcrete" specimen, respectively.

$$T = 2P/\pi ld \quad (1)$$

where T = splitting tensile strength, psi; P = maximum applied load indicated by the testing machine, lbf; l = length of the cylinder specimen, in; d = diameter of the cylinder specimen, in.

© 2026 by the author(s). Distributed under a Creative Commons CC BY license.

Preprints.org (www.preprints.org) | NOT PEER-REVIEWED | Posted: 6 August 2026 doi:10.20944/preprints202608.0409.v1

Figure 15. "Cobcrete" splitting cylinder test setup.

Figure 16. Fractured "cobcrete" cylinder.

© 2026 by the author(s). Distributed under a Creative Commons CC BY license.

Preprints.org (www.preprints.org) | NOT PEER-REVIEWED | Posted: 6 August 2026 doi:10.20944/preprints202608.0409.v1

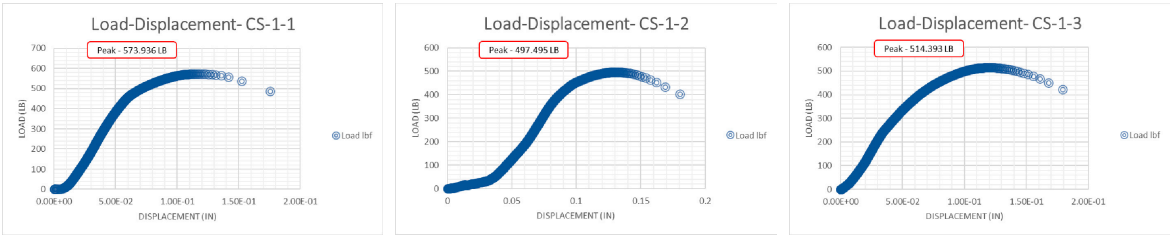

(1) **(2)** **(3)**

Figure 17. "Cobcrete" Load-Displacement graph from tests.

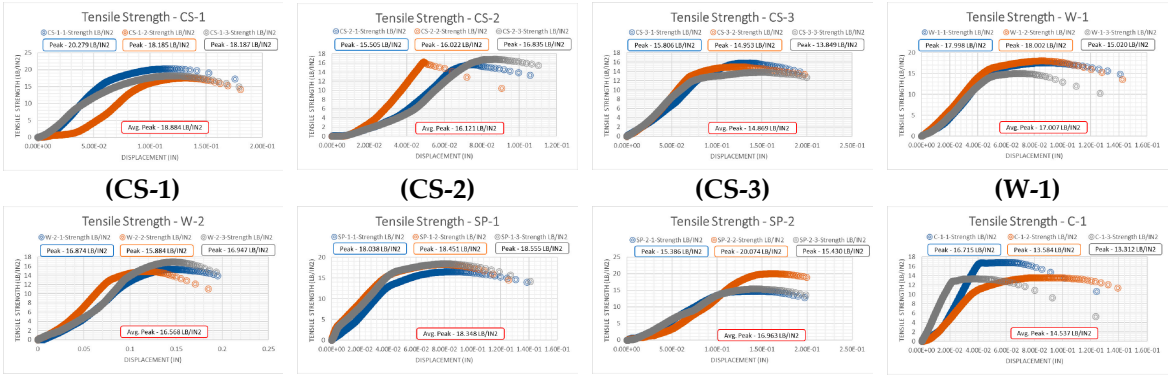

(CS-1) **(CS-2)** **(CS-3)** **(W-1)**

(W-2) **(SP-1)** **(SP-2)** **(C-1)**

Figure 18. "Cobcrete" tensile strength graph of various mixes.

2.4.4. Three-Point Bending Flexural Test of Cobcrete

The cobcrete beams were tested for flexural strength on the 28th day. For each specimen type, three samples were cast. Flexural strength was tested according to ASTM-C293/C293M [10,11].

The loading rate used in the testing machine was 76 lbf/min. From the testing machine, the basic raw data were collected: displacement, load, and time. Using the displacement and load data points, a Load-Displacement scattered graph is plotted for three different beams for each specimen, as shown in Figure 21. Finally, by using Equation (2), the Flexural Strength-Displacement graph is plotted, as shown in Figure 22, by combining the three graphs of the three samples of a specimen. Figures 19 and 20 show the test setup and the fractured "cobcrete" specimen, respectively.

$$R = 3PL/2b \quad (2)$$

where R = modulus of rupture or flexural strength, psi; P = maximum applied load indicated by the testing machine, lbf; L = span length, in; b = average width of specimen at the fracture, in; d = average depth of specimen at the fracture, in.

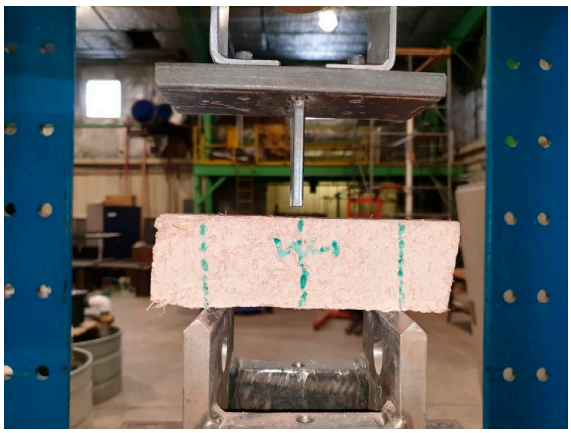

Figure 19. "Cobcrete" flexure test setup.

© 2026 by the author(s). Distributed under a Creative Commons CC BY license.

Preprints.org (www.preprints.org) | NOT PEER-REVIEWED | Posted: 6 August 2026 doi:10.20944/preprints202608.0409.v1

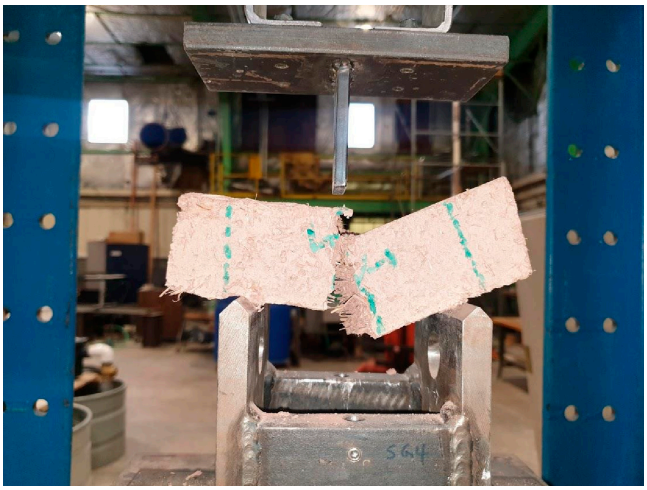

Figure 20. Fractured "cobcrete" rectangular beam.

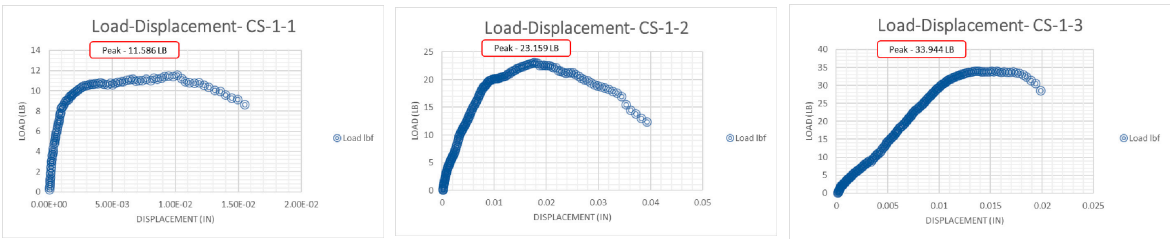

(1) **(2)** **(3)**

Figure 21. "Cobcrete" Load-Displacement graph.

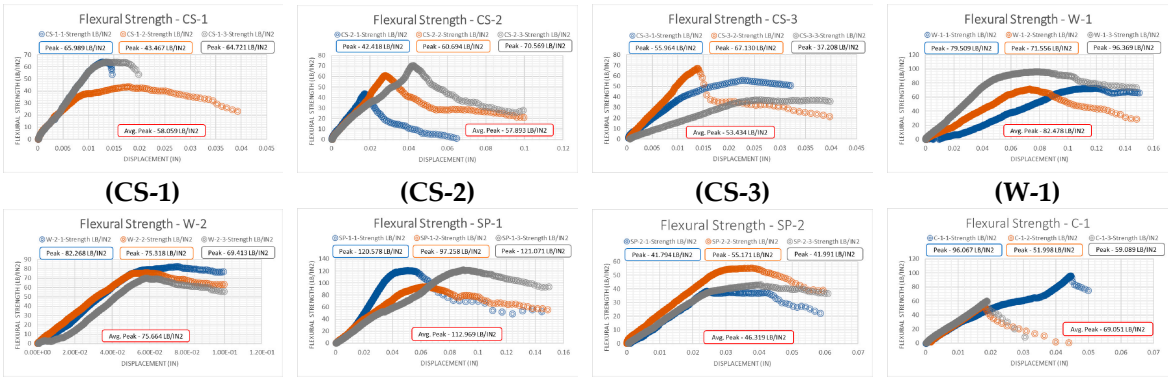

(CS-1) **(CS-2)** **(CS-3)** **(W-1)**

(W-2) **(SP-1)** **(SP-2)** **(C-1)**

Figure 22. "Cobcrete" 7th day flexural strength graph of various mixes.

2.4.5. Compressive Strength Test of Hempcrete

The hempcrete cubes were tested for the 7th day, 14th day, and 28th day strength comparison. For each age category, three samples were cast, resulting in a total of nine samples. The cubes' compressive strength was tested according to ASTM-C109/C109M [12].

The loading rate used in the testing machine was 70 lbF/min [13,14,44]. From the testing machine, three basic raw data points were collected: displacement, load, and time. By dividing the load by the cross-sectional area of the specimens, the Compressive Strength-Displacement graph is plotted, as shown in Figure 25. Figures 23 and 24 show the test setup and the fractured hempcrete specimen, respectively.

© 2026 by the author(s). Distributed under a Creative Commons CC BY license.

Preprints.org (www.preprints.org) | NOT PEER-REVIEWED | Posted: 6 August 2026 doi:10.20944/preprints202608.0409.v1

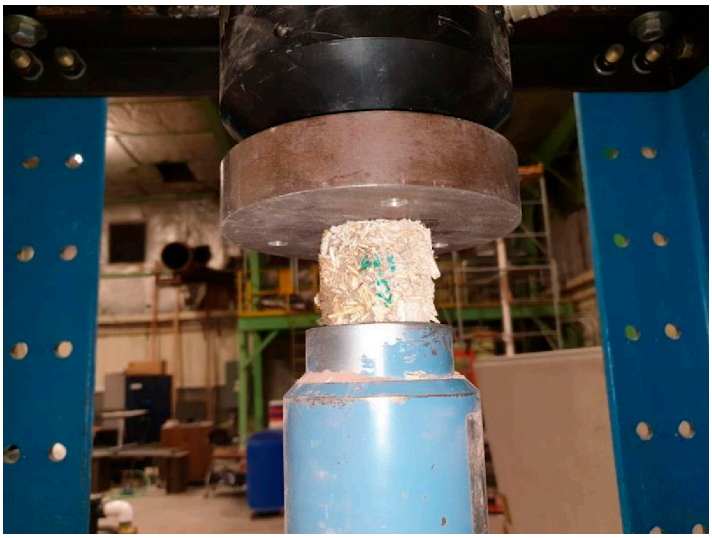

Figure 23. Hempcrete compression test setup.

Figure 24. Fractured hempcrete cube.

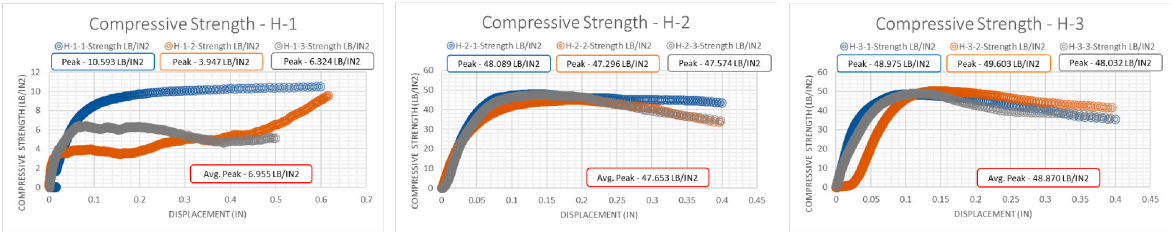

(H-1) **(H-2)** **(H-3)**

Figure 25. Hempcrete strength graph of various mixes.

2.5. Preparation for Manual 3D Printing

The 3D printing process of cobcrete has several parameters that need to be considered. The preparation commenced from mixing the material with the required mix ratio designs. Once the material was mixed, the 3D model of the structure was built in Rhino using a tool called Grasshopper. Since the printing process using the actual machine requires additional lab workers or students, manual printing was used to fully check the pumpability, printability, and buildability of the material [36]. For this initial experiment, manual printing is essentially pumping to extrude material using a hand-held syringe. Once the material was prepared, the extrusion process started by feeding the hand

© 2026 by the author(s). Distributed under a Creative Commons CC BY license.

Preprints.org (www.preprints.org) | NOT PEER-REVIEWED | Posted: 6 August 2026 doi:10.20944/preprints202608.0409.v1

pump with the material. Since the manual extruder was not operating automatically, manual pressing was required to assist in achieving a consistent flow rate [37, 45, 46]. Accordingly, the extruding process commenced from manually extruding two different mixtures using the syringe. These two prints helped provide insights on the printability and buildability of the structures, considering both the material property and printing setup. Thus, an additional six different mix ratios were designed and extruded manually using the hand pump with improved quality and printing setup, as shown in Figures 26 and 27.

Cobcrete' Mix Ratio Comparision (Weighted)													
	Mine (1)		Mine (2)		Mine (3)		Amnah			Gomaa		WASP	
Raw Material	%		%		%		%		%	Guess		%	
Clay	23	1.15	21.6	1.08	21	1.05	49	2.45		17	0.85	17	0.85
Sand	54	2.7	50.7	2.535	54	2.7	15.3	0.765	73	53	2.65	48	2.4
Lime	5	0.25	4.7	0.235	5	0.25	10	0.5		3	0.15	13	0.65
Water	17	0.85	22	1.1	19	0.95	24.2	1.21	25	25	1.25	20	1
Straw	1	0.05	1	0.05	1	0.05	1.5	0.075	2	2	0.1	1	0.05
Rice Husk - Hemp		0		0		0		0			0	1	0.05
Additive	0	0	0	0	0	0	0	0			0	0	0
Total	100	5	100	5	100	5	100	5	100	100	5	100	5
		5		5		5		5			5		5

Figure 26. Various Mix ratios.

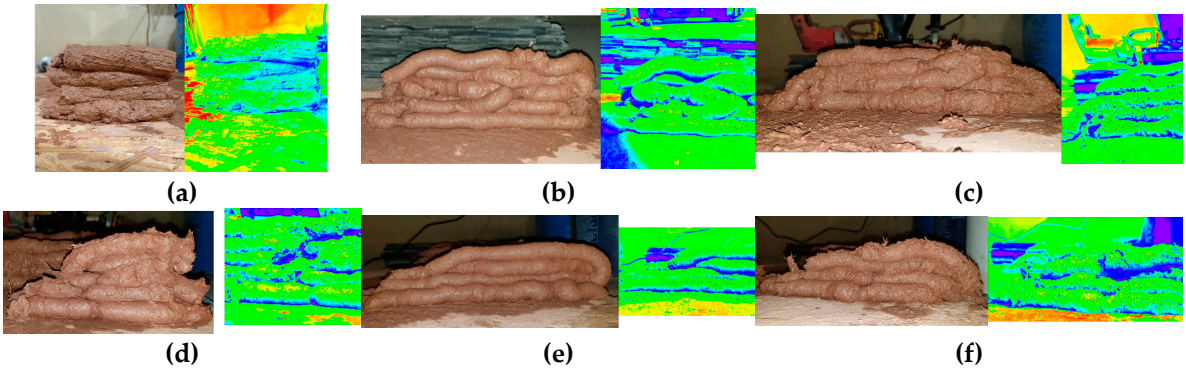

Figure 27. Mix ratio, extruded, and thermal images of (**a**) M-1, (**b**) M-2, (**c**) M-3, (**d**) A, (**e**) G, and (**f**) W, using manual pump.

3. Results and Discussion

3.1. Evaluation of the Mechanical Properties of 3D Printable Cobcrete

As per the results obtained from the compression test, it was observed that the compressive strength exhibited a decline with an increase in sand content. This decrease in strength was attributed to heightened material heterogeneity and the displacement of sand grains from the edges [39,40, 47, 48]. The pinnacle compressive strength value of 125 psi was achieved with a sand content of 63%. Conversely, an augmentation in water content, or moisture content, within the mixture led to a reduction in compressive strength. Specifically, as the water content decreased from 19% to 15%, the compressive strength surged from 126 psi to 158 psi.

Significantly, the experimental findings confirmed that the introduction of higher superplasticizer quantities yielded a marked enhancement in compressive strength. The progression from 0.5% to 1% and subsequently to 1.5% superplasticizer content corresponded to compressive strength values of 111 psi, 125 psi, and 216 psi, respectively. Additionally, the inclusion of 3% cement resulted in a notable boost in compressive strength, reaching 206 psi. Nevertheless, this increase did not surpass the compressive strength observed in specimens containing 1.5% superplasticizer.

Moving on to the outcomes derived from the splitting tensile test, the tensile strength of the specimens displayed minimal variability, ranging from 14 psi to 16 psi. It is noteworthy that all specimens maintained a consistent 1% straw content, underscoring the pivotal role of straw reinforcement content in influencing the tensile strength of the cobcrete.

© 2026 by the author(s). Distributed under a Creative Commons CC BY license.

Preprints.org (www.preprints.org) | NOT PEER-REVIEWED | Posted: 6 August 2026 doi:10.20944/preprints202608.0409.v1

In terms of the three-point bending flexure test, the flexural strength of the "cobcrete" beam demonstrated a direct correlation with reduced water content. Moreover, augmenting the superplasticizer content from 0.5% to 1.5% resulted in a substantial increase in flexural strength, escalating from 46 psi to 112 psi. Generally, the flexural strength of the "cobcrete" samples encompassed a range spanning 46 psi to 112 psi.

3.2. Evaluation of the Mechanical Properties of 3D Printable Hempcrete

Drawing upon the findings of the hempcrete compression test, a substantial reduction in compressive strength is observed with an increase in hemp content within the mixture. Notably, a decrease in hemp content from 24.5% to 6% yields a concurrent increase in compressive strength, elevating it from 6.9 psi to 48.8 psi. Moreover, there exists a positive correlation between the augmentation of lime content and the resultant increase in compressive strength. Broadly speaking, the compressive strength of hempcrete samples, evaluated on the 7th day, encompasses a range spanning from 6.9 psi to 48.8 psi.

3.3. Discussion on the Performance and Feasibility of 3D Printable Cobcrete

Based on the outcomes of the experimental study, mix ratios M-1, M-3, A, and W exhibit notable levels of buildability, as inferred from the procedures and material characteristics employed in the experimentation. In contrast, mix ratios M-2 and G display moderate buildability and limited cohesiveness. Following the first day of the extrusion process, mix ratio M-1 demonstrates a rapid increase in hardness. Conversely, mix ratios M-2, M-3, G, and W remain in a relatively moist state after the initial day of extrusion. In a broader context, mix ratio W showcases superior buildability, cohesiveness, and workability, rendering it a suitable candidate for the additive manufacturing of structural components. Figure 28 shows summary of all mix ratios observations.

"Cobcrete" Mix Ratio Comparison (Weighted Percentage)

	Mine (1)		Mine (2)		Mine (3)		Amnah		Gomaa			WASP	
Raw Material	%	kg	%	kg	%	kg	%	kg	%	Guess	kg	%	kg
Clay	23	1.15	21.6	1.08	21	1.05	49	2.45		17	0.85	17	0.85
Sand	54	2.7	50.7	2.535	54	2.7	15.3	0.765	73	53	2.65	48	2.4
Lime	5	0.25	4.7	0.235	5	0.25	10	0.5		3	0.15	13	0.65
Water	17	0.85	22	1.1	19	0.95	24.2	1.21	25	25	1.25	20	1
Straw	1	0.05	1	0.05	1	0.05	1.5	0.075	2	2	0.1	1	0.05
Rice Husk - Hemp		0		0		0		0			0	1	0.05
Additive	0	0	0	0	0	0	0	0			0	0	0
Total	100	5	100	5	100	5	100	5	100	100	5	100	5
		5		5		5		5			5		5
Right after extrusion					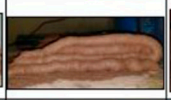								
Thermal Image	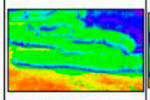		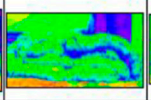		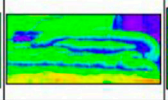		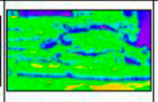		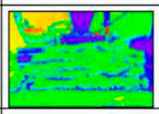			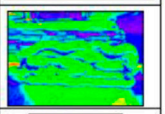	
1 day after extrusion					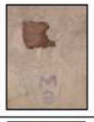								
1 day after extrusion after hand pressing													
	• Not deformed • Already hardened		• Deformed • Still wet		• Deformed • Still wet		• No deformation • Already hardened		• Deformed • Still wet			• Deformed • Still wet	
Observation	• High buildability • Consistent • Less workability		• Medium buildability • Less consistent • Medium workability		• High buildability • Consistent • Less void • High workability – extrudable		• High buildability • Consistent • Less workability (sticky)		• Medium buildability • Not consistent • Void • Medium workability			• High buildability • Consistent • Less void • High workability	

Figure 28. Observation of the six mix ratios.

© 2026 by the author(s). Distributed under a Creative Commons CC BY license.

Preprints.org (www.preprints.org) | NOT PEER-REVIEWED | Posted: 6 August 2026 doi:10.20944/preprints202608.0409.v1

3.4. Improved Mixture Design and Manual 3D Printing Trial

Drawing upon the results of the experimentation involving six distinct mix ratios, a novel composite ratio was formulated by incorporating hemp fibers into the composite constituents. Figure 29 provides a visual representation of the ingredient percentages and corresponding weights for a comprehensive 5 kg mixture design when employing a compact bowl mixer. In scenarios involving a larger drum mixer, the water quantity is adjusted to compensate for variables such as potential water loss during mixing, ensuring consistent results, as depicted in Figure 30. Furthermore, the time lapse and observation of the manual extrusion process for a small-scale wall are illustrated in Figures 31 and 32, respectively.

New Hemp-Lime Cobcrete Mix - small		
Raw Material	%	kg
Clay	**16**	0.80
Sand	**44**	2.20
Lime	**16**	0.80
Water	**20**	1.00
Hemp	**2**	0.10
Additive	**2**	0.10
Total	**100**	5
		5

Figure 29. Mix ratio and consistency of New Hemp-Lime Cobcrete when mixed in a small bowl.

New Hemp-Lime Cobcrete Mix - large		
Raw Material	%	kg
Clay	**15.7**	12.56
Sand	**43.2**	34.56
Lime	**15.7**	12.56
Water	**23.3**	18.64
Hemp	**2**	1.60
Additive	**0.1**	0.08
Total	**100**	80
		80

Figure 30. Mix ratio and consistency of New Hemp-Lime Cobcrete when mixed in a large drum mixer.

Printing Time/Layer Lapse - Initial

© 2026 by the author(s). Distributed under a Creative Commons CC BY license.

Preprints.org (www.preprints.org) | NOT PEER-REVIEWED | Posted: 6 August 2026 doi:10.20944/preprints202608.0409.v1

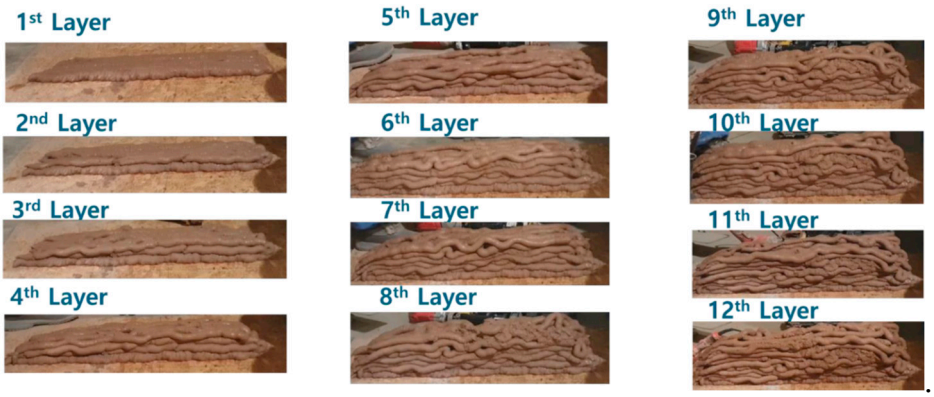

Figure 31. Extruded layers lapse.

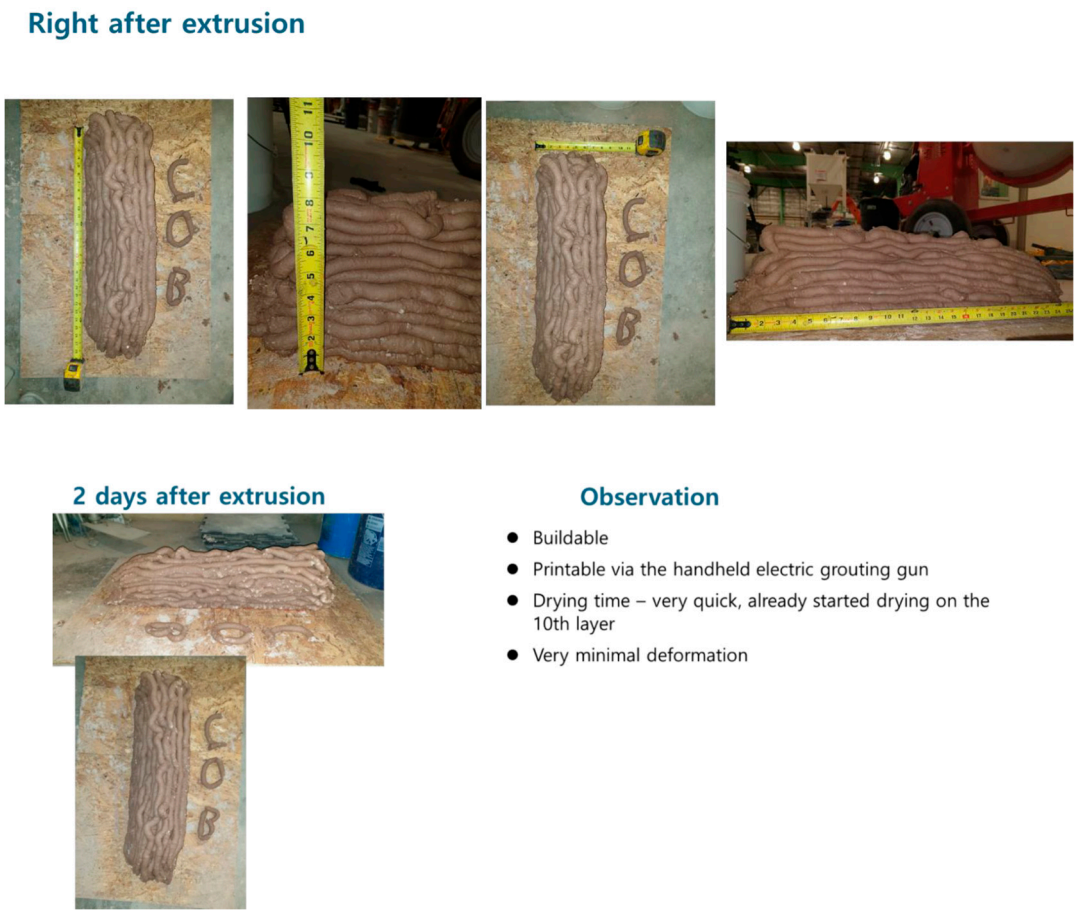

Figure 32. Manually extruded small wall.

4. Conclusions

The paper presents an initial study on the preparation and evaluation of printability of cobcrete and hempcrete materials. The authors focused on several aspects of the extrusion material, including evaluation of the extrusion process as a precursor of 3D printing, material properties, and mechanical performance. The study's key findings and conclusions are as follows.

The preparation process for manual extrusion of cobcrete involved mixing the material according to different mix ratio designs. The 3D model of the structure was generated using Rhino and Grasshopper software. The feasibility of 3D printing was explored using the extrusion process to assess the pumpability, printability, and buildability of the material. This involved using manual

© 2026 by the author(s). Distributed under a Creative Commons CC BY license.

Preprints.org (www.preprints.org) | NOT PEER-REVIEWED | Posted: 6 August 2026 doi:10.20944/preprints202608.0409.v1

extrusion, like a syringe and a hand pump, to deposit the material in controlled patterns. The extrusion process required manual assistance to ensure consistent flow rates, and this preliminary manual extrusion process served as a valuable insight into material behavior and printing setup.

Following the preparation and preliminary testing, the authors conducted an in-depth evaluation of the physical and mechanical properties of the 3D printable cobcrete and hempcrete materials. The evaluation covered various parameters, including compressive strength, tensile strength, and flexural strength.

For cobcrete:

- Compressive strength was affected by the sand content, with higher sand content leading to reduced strength due to heterogeneity and displacement of sand grains.
- Higher superplasticizer content improved compressive strength, with 1.5% yielding the highest strength.
- The inclusion of cement and reduced water content enhanced compressive strength.
- Tensile strength showed minimal variation, emphasizing the role of straw reinforcement.
- Flexural strength improved with reduced water content and higher superplasticizer content.

For hempcrete:

- Decreasing hemp content from 24.5% to 6% yields a concurrent increase in compressive strength, elevating it from 6.9 psi to 48.8 psi.
- Increasing lime content from 33% to 47.5% resulted in higher compressive strength, elevating it from 6.9 psi to 48.8 psi as well.
- Compressive strength in general varied across the tested hempcrete samples with different hemp and lime content.

In summary, the paper provides valuable insights into the potential for the 3D printing process of cobcrete and hempcrete materials, based on an initial extrusion study using a hand pump and syringe. It underscores the importance of material composition, mix ratios, and additive contents in influencing both physical and mechanical properties. The manual extrusion experimentation served as a practical approach to understanding the behavior of these materials for actual 3D printing using a robotic arm and an electric mixer and pumping system. Additionally, the paper highlights the potential for optimizing the properties of these materials through adjustments in mix design and additives. These findings contribute to the advancement of 3D printed construction materials and provide a foundation for further research and development in this field.

Author Contributions: Conceptualization, E.B. and A.M.M.; methodology, E.B.; software, E.B.; validation, E.B., A.M.M., G.U.; formal analysis, E.B.; investigation, E.B.; resources, A.M.M., G.U.; data curation, E.B.; writing—original draft preparation, E.B.; writing—review and editing, A.M.M., G.U.; visualization, E.B.; and supervision, A.M.M., G.U. All authors have read and agreed to the published version of the manuscript.

Funding: This research received funding from Schlumberger Foundation Faculty for the Future Fellowship Program.

Data Availability Statement: Data is contained within the article.

Acknowledgments: The authors gratefully acknowledge the Department of Architectural Engineering at The Pennsylvania State University for providing laboratory access and equipment used in this study and the Schlumberger Foundation Faculty for the Future Fellowship Program for providing a fellowship to the corresponding author.

Conflicts of Interest: The authors declare no conflicts of interest.

© 2026 by the author(s). Distributed under a Creative Commons CC BY license.

Preprints.org (www.preprints.org) | NOT PEER-REVIEWED | Posted: 6 August 2026 doi:10.20944/preprints202608.0409.v1

References

1. Alhumayani, H.; Gomaa, M.; Soebarto, V.; Jabi, W. Environmental assessment of large-scale 3D printing in construction: A comparative study between COB and concrete. J. Clean. Prod. 2020, 270, 122463.
2. Binega Yemesegen, E.; Memari, A.M. A review of experimental studies on COB, Hempcrete, and bamboo components and the call for transition towards sustainable home building with 3D printing. Constr. Build. Mater. 2023, 399, 132603.
3. Binega, E.; Memari, A.M. Learning from historical building construction in Sub-Saharan Africa to adapt for green 3D printing of houses. J. Green Build. 2023, 18, 3–28.
4. Binega, E.; Yang, L. Online geometry quality assessment during directed energy deposition metal additive manufacturing using laser line scanner. In Proceedings of the International Solid Freeform Fabrication Symposium, Austin, TX, USA, 2021.
5. Binega, E.; et al. Online geometry monitoring during directed energy deposition additive manufacturing using laser line scanning. Precis. Eng. 2022, 73, 104–114.
6. Ferretti, E.; et al. Mechanical properties of a 3D-printed wall segment made with an earthen mixture. Materials 2022, 15, 438.
7. 7. Gomaa, M.; Jabi, W.; et al. 3D printing system for Earth-based construction: Case study of cob. Autom. Constr. 2021, 124, 103577.
8. Gomaa, M.; Vaculik, J.; et al. Feasibility of 3DP cob walls under compression loads in low-rise construction. Constr. Build. Mater. 2021, 301, 124079.
9. Haddad, K.; Latif, E.; Lannon, S. The state of the art of COB construction: A comprehensive review of the optimal mixtures and testing methods. RILEM Bookseries 2023, 212–231.
10. Hamard, E.; et al. Cob, a vernacular earth construction process in the context of modern sustainable building. Build. Environ. 2016, 106, 103–119.
11. Alqenaee, A.; Memari, A. Experimental study of 3D printable cob mixtures. Constr. Build. Mater. 2022, 324, 126574.
12. Jami, T.; Rawtani, D.; Agrawal, Y.K. Hemp concrete: Carbon-negative construction. Emerg. Mater. Res. 2016, 5, 240–247.
13. Kinnane, O.; et al. Acoustic absorption of hemp-lime construction. Constr. Build. Mater. 2016, 122, 674–682.
14. Miccoli, L.; Müller, U.; Fontana, P. Mechanical behaviour of earthen materials: A comparison between earth block masonry, rammed earth, and cob. Constr. Build. Mater. 2014, 61, 327–339.
15. Sinka, M.; et al. Hempcrete – CO2 neutral wall solutions for 3D printing. Environ. Clim. Technol. 2022, 26, 742–753.
16. Vinceslas, T.; et al. Further development of a laboratory procedure to assess the mechanical performance of cob. Environ. Geotech. 2020, 7, 200–207.
17. Yadav, M.; Saini, A. Opportunities and challenges of hempcrete as a building material for construction: An overview. Mater. Today Proc. 2022, 65, 2021–2028.
18. Eberhard, D.; Novara, J.; Popovec, B. Cob: A Sustainable Building Material. Civil Engineering Senior Theses 66, Santa Clara University, 2018.
19. Concrete Construction Staff. Relationship between Seven- and 28-Day Strengths. Available online: https://www.concreteconstruction.net/how-to/relationship-between-seven-and-28-day-strengths_o (accessed on 3 September 2023).
20. Zavaleta, D.; et al. Additive construction using enhanced earthen-based composites: Improvement of the mechanical strength and water durability using chitosan and agave fibers. Constr. Build. Mater. 2024, 411, 134159.
21. Ji, Y.; Poullain, P.; Leklou, N. The selection and design of earthen materials for 3D printing. Constr. Build. Mater. 2023, 404, 133114.
22. Sinka, M.; et al. Fast setting binders for application in 3D printing of bio-based building materials. Sustainability 2020, 12, 8838.
23. de Bruijn, P.; Johansson, P. Moisture fixation and thermal properties of lime–hemp concrete. Constr. Build. Mater. 2013, 47, 1235–1242.

© 2026 by the author(s). Distributed under a Creative Commons CC BY license.

Preprints.org (www.preprints.org) | NOT PEER-REVIEWED | Posted: 6 August 2026 doi:10.20944/preprints202608.0409.v1

24. Nguyen, T.-T.; et al. Influence of compactness and hemp hurd characteristics on the mechanical properties of lime and hemp concrete. Rev. Eur. Genie Civ. 2009, 13, 1039–1050.
25. Rahul, A.V.; et al. Mechanical characterization of 3D printable concrete. Constr. Build. Mater. 2019, 227, 116710.
26. Oya, A. Effect of rice straw length on mechanical properties of quick lime and rice husk ash stabilized soil. Int. J. GEOMATE 2016, 21, 5193.
27. Walker, R.; Pavia, S.; Mitchell, R. Mechanical properties and durability of hemp-lime concretes. Constr. Build. Mater. 2014, 61, 340–348.
28. Li, X. Physical, Chemical, and Mechanical Properties of Bamboo and Its Utilization Potential for Fiberboard Manufacturing. Master's Thesis, Louisiana State University, 2004.
29. Alhumayani, H.; Gomaa, M.; Soebarto, V.; Jabi, W. Environmental assessment of large-scale 3D printing in construction: A comparative study between COB and concrete. J. Clean. Prod. 2020, 270, 122463.
30. Arnaud, L.; Gourlay, E. Experimental study of parameters influencing mechanical properties of hemp concretes. Constr. Build. Mater. 2012, 28, 50–56.
31. Walker, R. A Study of the Properties of Lime-Hemp Concrete with Pozzolans. Ph.D. Thesis, Trinity College Dublin, 2013.
32. Review of hempcrete as a sustainable building material. Int. J. Archit. Eng. Constr. 2021, 10.
33. van Hierden, N.Z.; et al. Use of hemp fibres in 3D printed concrete. Constr. Technol. Archit. 2022, 1, 758–765.
34. Rocha, D.; Faria, P.; Lucas, S.S. Additive manufacturing of earth-based materials: A literature review on mortar composition, extrusion, and processing earth. Materials 2023, 17, 202.
35. Faleschini, F.; et al. Sustainable mixes for 3D printing of earth-based constructions. Constr. Build. Mater. 2023, 398, 132496.
36. Li, S.; et al. Robotics in 3D concrete printing. In Automation in Construction toward Resilience; CRC Press: Boca Raton, FL, USA, 2023; pp. 27–42.
37. Veliz Reyes, A.; et al. Computing craft – early stage development of a robotically-supported 3D printing system for COB structures. In Proceedings of the eCAADe, 2018.
38. Wu, X.; et al. Experimental Study on Buildability and Mechanical Properties of 3D Printing Cob (preprint), 2023.
39. Faes, M.; et al. Extrusion-based 3D printing of ceramic components. Procedia CIRP 2015, 28, 76–81.
40. Zuo, Z.; et al. Experimental research on transition from scale 3D printing to full-size printing in construction. Constr. Build. Mater. 2019, 208, 350–360.
41. Xiao, J.; et al. Large-scale 3D printing concrete technology: Current status and future opportunities. Cem. Concr. Compos. 2021, 122, 104115.
42. Dalbiso, A.D.; Nuramo, D.A. Ethiopian vernacular bamboo architecture and its potentials for adaptation in modern urban housing: A case study. In Modern Engineered Bamboo Structures; CRC Press: Boca Raton, FL, USA, 2019; pp. 91–98.
43. Kathir. Bamboo for Reinforced Concrete Construction. Civil Snapshot, 2019. Available online: https://civilsnapshot.com/bamboo-for-reinforced-concrete-construction/(accessed on 31 January 2023).
44. Yemesegen, E.B. Material Science, Analysis, and Design of Clay-Hemp Based Material Mixtures for Sustainable Home Building Using 3D Printing Technology. Ph.D. Dissertation, The Pennsylvania State University, University Park, PA, USA, 2024.
45. Yemesegen, E.B.; Memari, A.M. 3D Printing of “Clay-Hemp” Sustainable Structures for Residential Construction. Proceedings of the 7th Residential Building Design & Construction Conference (RBDCC), The Pennsylvania State University, University Park, PA, USA, 2024.
46. Yemesegen, E.B.; Memari, A.M. Incorporating Carbon-Negative Hempcrete in 3D-Printed Eco-Friendly Residential Houses. Proceedings of the 7th Residential Building Design & Construction Conference (RBDCC), The Pennsylvania State University, University Park, PA, USA, 2024.

© 2026 by the author(s). Distributed under a Creative Commons CC BY license.

Preprints.org (www.preprints.org) | NOT PEER-REVIEWED | Posted: 6 August 2026 doi:10.20944/preprints202608.0409.v1

47. Yemesegen, E.B; Memari, A.M. 3D Printing of Residential Houses by Adapting the Historical African Sustainable Housings. Proceedings of the 2022 Residential Building Design & Construction Conference (RBDCC), The Pennsylvania State University, University Park, PA, USA, 2022.
48. Yemesegen, E.B.; Memari, A.M. Advancing Sustainable Construction: Robotic 3D Printing and Failure Analysis of Clay-Hemp Composite Structural Walls. Proceedings of the 8th Residential Building Design & Construction Conference (RBDCC), The Pennsylvania State University, University Park, PA, USA, 2026.:

Disclaimer/Publisher's Note: The statements, opinions and data contained in all publications are solely those of the individual author(s) and contributor(s) and not of MDPI and/or the editor(s). MDPI and/or the editor(s) disclaim responsibility for any injury to people or property resulting from any ideas, methods, instructions or products referred to in the content.

© 2026 by the author(s). Distributed under a Creative Commons CC BY license.